Nanometer resolution piezoresponse force microscopy to study deep submicron ferroelectric and ferroelastic domains

Yachin Ivry,[1] DaPing Chu,[2] and Colm Durkan[1,a)]
[1]*Nanoscience Centre, University of Cambridge, 11 JJ Thomson Avenue, Cambridge CB3-0FF, United Kingdom*
[2]*Electrical Engineering Division, University of Cambridge, 9 JJ Thomson Avenue, Cambridge CB3-0FA, United Kingdom*

(Received 16 September 2008; accepted 4 March 2009; published online 22 April 2009)

Understanding ferroelectricity at the deep submicron regime is desirable in utilizing it for next generation nonvolatile memory devices, medical imaging systems, and rf filters. Here we show how piezoresponse force microscopy can be enhanced (1 nm resolution). Using this method, we have investigated ferroelectric and ferroelastic domains at the deep submicron regime in polycrystalline lead zirconium titanate thin films. We demonstrate that in the clamped films, periodic pairs of 90° domains are stable even at 10 nm width, challenging recent predictions of minimum domain size, and suggesting ferroelectricity for high-density storage devices (≥10 Tbyte/in^2). © *2009 American Institute of Physics*. [DOI: 10.1063/1.3105942]

High-density nonvolatile memories constitute a high-potential arena. Ferroelectric-based memories are currently one of the leading candidates for such devices.[1] Ferroelectrics are widely used in everyday technologies such as rf filters and medical imaging systems.[2,3] Although ferroelectricity has been extensively studied at both the macroscopic (>1 μm) and atomic scale (<1 nm),[4,5] the relation between the behavior at these two scales is still poorly understood.[6–8] Furthermore, during the past half century, many attempts have been made to predict the minimum dimensions for a ferroelectric domain while experimental observations continually challenge them.[9–12] It has already been shown that ferroelectricity can exist even in films 3 unit cells thick.[13] Nonetheless, there is still uncertainty concerning the minimum lateral dimensions below which a stable ferroelectric, or ferroelastic domain cannot exist.[14] Piezoresponse force microscopy (PFM) is a nondestructive method that uses atomic force microscopy (AFM) to image the in-plane and out-of-plane polarization distribution simultaneously with the topography in piezoelectrics (and therefore in ferroelectrics).[14–17] As a result of the applied ac voltage, between the AFM tip and the bottom electrode, at a frequency f_{ac}, the AFM cantilever oscillates at f_{ac} due to three independent mechanisms: (a) the inverse piezoelectric effect, (b) local electrostatic interactions at the tip-surface contact point, and (c) nonlocal electrostatic interactions between the cantilever and the sample surface.[14] Since both piezoelectricity and ferroelectricity are collective phenomena, in which the strain is evenly distributed among columnar unit cells (*body force effect*),[5,18] the measured surface polarization reliably reflects also the microscale polarization distribution. If electrostatic forces govern the cantilever oscillations, the PFM image will reflect either the charge that screens the polarization or the polarization itself.[19–21] While AFM can be used down to the atomic regime, the reproducible lateral resolution obtained by PFM is currently far from being so. We have enhanced the sensitivity of standard PFM to result in high-resolution (≤1 nm) polarization imaging. We chose to examine thin polycrystalline lead zirconium titanate (PZT) films, which have a strong piezoresponse and are a mainstream material in ferroelectric-based technologies. As discussed in the supplemental material, the samples under examination were predominantly (110) (Fig. S1), 190 nm thick, sol-gel deposited on a bottom electrode, similar to the way described elsewhere,[15] and with the composition $PbZr_{0.3}Ti_{0.7}O_3$.

Most works in the field of PFM address local quantitative analyses,[22] while not much has been done to optimize the spatial resolution of the technique despite the great interest in detecting and manipulating ferroelectricity at the intermediate scale.[23] To increase the resolution of PFM, one should increase the signal to noise ratio of the cantilever's oscillation. One possible way is to increase the applied voltage while insuring that this does not change the polarization. Hence, most studies involve voltages that correspond to an electric field smaller than the dc coercive field that flips the polarization.

The macroscopic dc coercive field of our samples is 35–40 kV cm^{-1}, whereas with PFM, ferroelectric patterns are formed with a dc voltage $V_{dc}^{coercive} \geq 3$ V, corresponding to an electric field of several hundred kV cm^{-1}.[15,23] However, when the writing time pulse is shorter than a certain time constant $\tau_{dc}^{writing}$ ($\sim$0.5 s in the studied samples), no patterns are written even with somewhat higher voltages.[15,23] Thus, one can deduce that applying higher rms ac voltages (V_{ac}) at $f_{ac} \gg 1/\tau_{dc}^{writing}$ should not affect the native polarization distribution. In the absence of permanent top electrodes, the writing time constant is associated with the screening charge accumulated on the sample's surface to stabilize the polarization of the film ($\sim$1 s).[24] This process is significantly slower than the actual polarization reversal ($\sim 10^{-12}$ s), imposed by the phonon speed in the material. Indeed, no significant differences were observed in more than fifty repeated scans, lasting several days, when $V_{ac} > 2 \times V_{dc}^{coercive}$ at $f_{ac} \gg 2$ Hz.

We used soft cantilevers (Pt/Cr coated ContE of Budget-Sensors, resonant frequency: 11–14 kHz, nominal force constant: 0.2 N m^{-1}). It has been shown that if strong forces are

[a)]Electronic mail: cd229@eng.cam.ac.uk.

 © 2009 American Institute of Physics

Downloaded 08 May 2009 to 133.28.47.30. Redistribution subject to AIP license or copyright; see http://apl.aip.org/apl/copyright.jsp

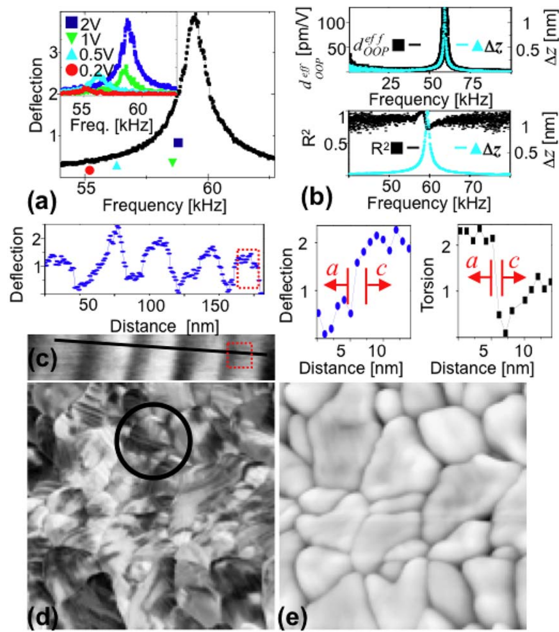

FIG. 1. (Color online) High-resolution PFM. (a) Main graph—the symmetric dependence of cantilever deflection on f_{ac} around f_{1res}^{ic} (V_{ac}=5 V) and the increase in resonance frequency with modulating voltage (small graph and symbols on main graph). (b) Comparing the dependence of d_{OOP}^{eff} (top) and R^2 (bottom) on f_{ac} to that of Δz reveals that the former behaves similarly to Δz and enhanced to ~2–3 times than the intrinsic value at $f_{ac}=f_{1res}^{ic}$. The highest linearity is obtained at $f_{ac}=f_{R^2}^{max}<f_{1res}^{ic}$. (c) A cross section (top left) of an out-of-plane polarization image of a polytwinned area (185×35 nm^2, bottom left) shows the sensitivity of the method. A closer look at both the out-of-plane (middle) and in-plane (right) cross sections from that area (designated by dashed squares) demonstrates ≤1 nm resolution around 90° domain walls. (d) PFM mapping reveals the coexistence of ferroelectric (shaded) and ferroelastic (striped) domains (***a-a*** twins are highlighted), (e) the simultaneous AFM topography image of the same area (2.2×2.2 μm^2).

applied to the cantilever (≥~1 μN, which usually corresponds to levers with ≥~10 N m^{-1} spring constant[14]), the inverse piezoelectric effect governs the cantilever's oscillations; whereas for lower forces, electrostatic forces should also be taken into account.[19,25] Kalinin and Bonnell[25] have demonstrated[19] that if the nonlocal electrostatic forces are dominant, the cantilever's first in-contact resonance frequency (f_{1res}^{ic}) should be 4.4 times higher than that of the free cantilever. Indeed, Fig. 1(a) shows that f_{1res}^{ic}=~55–60 kHz, in agreement with this determination. This is as opposed to the case where local electrostatic interactions dominate, in which case f_{1res}^{ic} is expected to be an order of magnitude higher. In the latter case, the resulting tip-surface repulsion force can overcome the adhesion so that the tip occasionally leaves the surface. If so, one would expect a nonlinear dependence of the measured cantilever deflection (Δz) as a function of applied voltage and an asymmetric dependence of Δz on frequency. On the other hand, if nonlocal electrostatic interactions govern the oscillations, the tip can still be kept in-contact, while the electrostatic interactions act on the cantilever like a homogeneous load, causing it to bow.[19] Therefore, a constant (const) is added to the out-of-plane piezoelectric constant (d_{OOP}), increasing the effective piezoresponse $d_{OOP}^{eff}=d_{OOP}+\text{const}$. This has the effect of increasing the measured cantilever's oscillations while the tip actually remains in contact, as $\Delta z=d_{OOP}^{eff}\times V_{ac}$.

The measured symmetric curve of Δz as a function of f_{ac} [Fig. 1(a)] further validates the Hertzian approximation, guaranteeing that small changes in force between the tip and sample are linear. To explore the interplay between the electrostatic interactions and the piezoresponse, we fitted Δz as a function of V_{ac} to a linear curve, extracting the effective piezoelectric coefficient d_{OOP}^{eff} as a function of f_{ac}. Moreover, we used R^2—the statistical value of the best fit, as the linearity figure of merit. Figure 1(b) shows that d_{OOP}^{eff} and Δz share a resonance at 59.45 kHz and behave similarly as a function of frequency, so that a enhances d_{OOP} to d_{OOP}^{eff} =170 pm/V, which is approximately two to three times higher than d_{OOP}.[19] On the other hand, it shows that the linearity of the piezoresponse (R^2) is well defined only close to f_{1res}^{ic}, and reaches a maximum at a frequency $f_{R^2}^{max}$ ≈57.8–58.6 kHz. That is near $f_{R^2}^{max}$, the electrostatic interactions enhance d_{OOP}^{eff}, on one hand, whereas on the other hand, they are too small to distort the piezoelectric linearity. Indeed, the highest resolution imaging was obtained near $f_{ac}=f_{R^2}^{max}$, whereas further from $f_{R^2}^{max}$ (including at $f_{ac}=f_{1res}^{ic}$), not only does the resolution decrease, but also the imaging is not always reproducible, suggesting the existence of local interactions comparable with the adhesion.

The nature of the cantilever oscillations associates them with atomic force acoustic microscopy (AFAM). In AFAM, the cantilever is in-contact with a sample that is oscillated close to f_{1res}^{ic}, which in turn depends on the applied force.[26,27] From a PFM perspective, choosing f_{ac} close to f_{1res}^{ic} means only increasing Δz, and hence the signal to noise ratio. However, the validity of the AFAM framework [Fig. 1(a)] carries the advantage of a comprehensive quantitative analysis capability.[26] In AFAM, when the cantilever is oscillated near f_{1res}^{ic}, its deflection is sensitive also to changes in local elasticity moduli (due to, e.g., crystallographic domain variations).[28] Nonetheless, since the only driving force is electric and the deflection signal is linear with applying force, the piezoelectric treatment, i.e., the usage of d_{OOP}^{eff} is justified. Moreover, although presumably, f_{1res}^{ic} may change during the scan,[17] the contrast reproducibility and high resolution imply that the change is small and reproducible with respect to the scanned area.

To obtain high-resolution imaging of the polarization distribution in the PZT films, we applied V_{ac}=0.2–5 V_{rms} between the cantilever and the bottom electrode, at $f_{ac}=f_{R^2}^{max}$, while recording the first harmonic locked-in signal. Figure 1(c) shows a cross section taken from a domain boundary, indicating ≤1 nm resolution for both out-of-plane and in-plane imaging[19]; whereas it should be noted that the resolution decreases with decreasing voltage and at frequencies further from $f_{R^2}^{max}$.

The imaging reveals two types of pattern: (i) randomly distributed shaded patterns with ~10 nm–1 μm typical diameter, and (ii) bundles of 10–40 aligned stripes with an alternating contrast and ~5–70 nm width [Figs. 1(d) and 1(e)]. We associate the random patterns with the native 180° ferroelectric domains; whereas the strict orientation of the latter suggests they are ferroelastic twins (*polytwins*), i.e., periodic elastic domains that arise to reduce the elastic energy by releasing strain with the polar axis in- and out-of-plane (~45°), respectively.[29] Based on the (110) tetragonality dominancy, these polytwins can be treated as $\ldots a/c/a/c\ldots$. Similarly, areas with polytwin arrays that are perpendicular to each other correspond to $\ldots \boldsymbol{a}_1/\boldsymbol{c}/\boldsymbol{a}_1/$

Downloaded 08 May 2009 to 133.28.47.30. Redistribution subject to AIP license or copyright; see http://apl.aip.org/apl/copyright.jsp

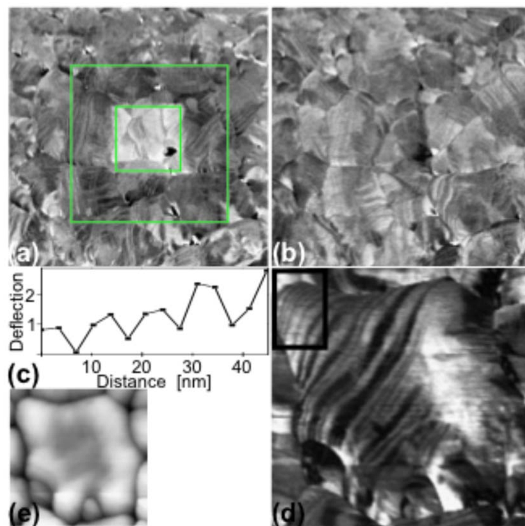

FIG. 2. (Color online) Ferroelasticity in thin PZT films. After manipulating the area (3×3 μm^2), striped domains appear in the simultaneous (a) out-of-plane and (b) in-plane PFM images. Whereas artificially patterned antiparallel domains are seen as shaded patterns only in the out-of-plane polarization image, showing the distinction between ferroelectric and ferroelastic domains. (c) A cross section of (d) the out-of-plane PFM image of an individual grain demonstrates a large-scale periodicity of 10 nm width for a single a/c period. (e) The topography of the same area (490×490 nm^2).

$-c/a_2/c/a_2\ldots$ ('*a-a*') twins [highlighted by the circle in Fig. 1(e)]. This association is supported by the fact that we measured the contrast between adjacent stripes (c^+ and a or c^- and a) to be of about half the value of the contrast between adjacent shaded patterns (c^+ and c^-). Moreover, in areas where the stripes continue through adjacent shaded domains of opposite contrast, the contrast is opposite (c^+ and c^- domains) only at every other stripe, whereas it is constant at the others (a domains).[30] Finally, these patterns have also been observed with the independent method of in-lens scanning electron microscopy in Fig. S2.

To further confirm this distinction, we first "wrote" antiparallel c domains by scanning a $2\times2\mu^2$ area while applying 10 V (dc only) between the tip and the bottom electrode, followed by a scan of a smaller area while applying −10 V. The written patterns appeared as shaded domains and were detected only in the out-of-plane images and not in the in-plane images, whereas the same stripes appeared in both images, verifying that stripes are 90° twins and shades are 180° domains [Figs. 2(a) and 2(b)].[31]

Recent studies claim that the smallest possible ferroelastic periodicity is ~27 nm.[32,33] The polytwin structure in Figs. 2(c) and S3 demonstrates a native ferroelastic periodicity of ~10 nm (i.e., ~24–26 unit cells). Therefore, this suggests a possibility of using ferroelectrics as memory elements with a density as high as >10 Tbyte/in.^{2}.[1,33] Since the grains in the film are columnar, the corresponding aspect ratio is higher than 35 with a ~5° corrugation angle at the PZT–Pt interface.[33] The high corrugation angle indicates strong local strain,[34] suggesting that it can exist only where this strain cannot be released otherwise, e.g., far away from sample edges where the substrate clamping is high. This explains why the short periodicity is not likely to be seen in single crystals and with TEM.[35]

To conclude, we have demonstrated that AFM can yield high-resolution out-of-plane and in-plane polarization-distribution imaging (≤1 nm) under ambient conditions. This is achieved by applying V_{ac} higher than the dc coercive field, near the cantilever's in-contact resonance frequency. Moreover, we extracted a new upper limit for the smallest ferroelastic domains.

[1] J. F. Scott, Science **315**, 954 (2007).
[2] M. Dawber, K. M. Rabe, and J. F. Scott, Rev. Mod. Phys. **77**, 1083 (2005).
[3] N. Setter, D. Damjanovic, L. Eng, G. Fox, S. Gevorgian, S. Hong, A. Kingin, H. Kohlstedt, N. Y. Park, G. B. Stephenson, I. Stolitchnov, A. K. Tagantsev, D. V. Taylor, T. Yamada, and S. Streiffer, J. Appl. Phys. **100**, 051606 (2006).
[4] C. L. Jia, S. B. Mi, K. Urban, I. Vrejoiu, B. Alexe, and D. Hesse, Nature Mater. **7**, 57 (2008).
[5] F. Jona and G. Shirane, *Ferroelectric Crystals* (Dover, New York, 1993).
[6] J. Y. Li, R. C. Rogan, E. Ustundag, and K. Bhattacharya, Nature Mater. **4**, 776 (2005).
[7] R. Ramesh and D. G. Schlom, Science **296**, 1975 (2002).
[8] Y. Ivry, V. Lyahovitskaya, I. Zon, I. Lubomirsky, E. Wachtel, and A. L. Roytburd, Appl. Phys. Lett. **90**, 172905 (2007).
[9] A. V. Bune, V. M. Fridkin, S. Ducharme, L. M. Blinov, S. P. Palto, A. V. Sorokin, S. G. Yudin, and A. Zlatkin, Nature (London) **391**, 874 (1998).
[10] D. R. Callaby, J. Appl. Phys. **37**, 2295 (1966).
[11] J. Junquera and P. Ghosez, Nature (London) **422**, 506 (2003).
[12] V. Nagarajan, S. Prasertchoung, T. Zhao, H. Zheng, J. Ouyang, R. Ramesh, W. Tian, X. Q. Pan, D. M. Kim, C. B. Eom, H. Kohlstedt, and R. Waser, Appl. Phys. Lett. **84**, 5225 (2004).
[13] D. D. Fong, G. B. Stephenson, S. K. Streiffer, J. A. Eastman, O. Auciello, P. H. Fuoss, and C. Thompson, Science **304**, 1650 (2004).
[14] M. Alexe, C. Harnagea, A. Visinoiu, A. Pignolet, D. Hesse, and U. Gosele, Scr. Mater. **44**, 1175 (2001).
[15] C. Durkan, M. E. Welland, D. P. Chu, and P. Migliorato, Phys. Rev. B **60**, 16198 (1999).
[16] A. Gruverman, O. Auciello, and H. Tokumoto, J. Vac. Sci. Technol. B **14**, 602 (1996).
[17] S. Jesse, B. Mirman, and S. V. Kalinin, Appl. Phys. Lett. **89**, 3 (2006).
[18] W. G. Cady, *Piezoelectricity: An Introduction to the Theory and Applications of Electromechanical Phenomena in Crystals* (Dover, New York, 1964).
[19] *Nanoscale Characterisation of Ferrorlectric Materials*, edited by M. Alexe and A. Gruverman (Springer, Heidelberg, 2004).
[20] J. W. Hong, S. I. Park, and Z. G. Khim, Rev. Sci. Instrum. **70**, 1735 (1999).
[21] T. Jungk, A. Hoffmann, and E. Soergel, Appl. Phys. Lett. **89**, 042901 (2006).
[22] S. Jesse, H. N. Lee, and S. V. Kalinin, Rev. Sci. Instrum. **77**, 073702 (2006).
[23] C. Durkan, D. P. Chu, P. Migliorato, and M. E. Welland, Appl. Phys. Lett. **76**, 366 (2000).
[24] C. S. Ganpule, A. L. Roytburd, V. Nagarajan, B. K. Hill, S. B. Ogale, E. D. Williams, R. Ramesh, and J. F. Scott, Phys. Rev. B **65**, 014101 (2001).
[25] S. V. Kalinin and D. A. Bonnell, Phys. Rev. B **65**, 125408 (2002).
[26] U. Rabe, S. Amelio, E. Kester, V. Scherer, S. Hirsekorn, and W. Arnold, Ultrasonics **38**, 430 (2000).
[27] U. Rabe, M. Kopycinska, S. Hirsekorn, J. M. Saldana, G. A. Schneider, and W. Arnold, J. Phys. D **35**, 2621 (2002).
[28] R. Nath, Y. H. Chu, N. A. Polomoff, R. Ramesh, and B. D. Huey, Appl. Phys. Lett. **93**, 072905 (2008).
[29] A. L. Roitburd, Phys. Status Solidi A **37**, 329 (1976).
[30] *a* and *c* refer to the out-of-plane imaging and should be swapped in the case of in-plane imaging.
[31] A. Hoffmann, T. Jungk, and E. Soergel, Rev. Sci. Instrum. **78**, 016101 (2007).
[32] J. S. Speck and W. Pompe, J. Appl. Phys. **76**, 466 (1994).
[33] A. H. G. Vlooswijk, B. Noheda, G. Catalan, A. Janssens, B. Barcones, R. Rijnders, D. H. A. Blank, S. Venkatesan, B. Kooi, and J. T. M. de Hosson, Appl. Phys. Lett. **91**, 112901 (2007).
[34] A. Schilling, T. B. Adams, R. M. Bowman, J. M. Gregg, G. Catalan, and J. F. Scott, Phys. Rev. B **74**, 024115 (2006).
[35] See EPAPS Document No. E-APPLAB-94-062912 for the supplementary figures. For more information on EPAPS, see http://www.aip.org/pubservs/epaps.html.

Downloaded 08 May 2009 to 133.28.47.30. Redistribution subject to AIP license or copyright; see http://apl.aip.org/apl/copyright.jsp